

DOI: 10.5586/asbp.3584

**Publication history**

Received: 2018-03-19

Accepted: 2018-05-17

Published: 2018-06-29

**Handling editor**

Beata Zagórska-Marek, Faculty of Biological Sciences, University of Wrocław, Poland

**Authors' contributions**

GJ: supervised the project, designed the experiments, analyzed the experimental data, and wrote the paper; AL: participated in designing the experiments, analyzing the experimental data, and writing the paper; TW: performed the experiments, analyzed the experimental data, and participated in writing the paper; MA, PJ, FM, LM, and RL: performed the experiments and analyzed the experimental data; MA and PJ contributed equally to this work

**Funding**

This work was supported by the Polish National Science Center based on decision number DEC-2013/09/B/NZ3/00449.

**Competing interests**

No competing interests have been declared.

**Copyright notice**

© The Author(s) 2018. This is an Open Access article distributed under the terms of the [Creative Commons Attribution License](https://creativecommons.org/licenses/by/4.0/), which permits redistribution, commercial and noncommercial, provided that the article is properly cited.

**Citation**

Adamiec M, Jagodzick P, Wyka TP, Ludwików A, Mituła F, Misztal L, et al. Chloroplast protease/chaperone AtDeg2 influences cotyledons opening and reproductive development in *Arabidopsis*. *Acta Soc Bot Pol*. 2018;87(2):3584. <https://doi.org/10.5586/asbp.3584>

**Digital signature**

This PDF has been certified using digital signature with a trusted timestamp to assure its origin and integrity. A verification trust dialog appears on the PDF document when it is opened in a compatible PDF reader. Certificate properties provide further details such as certification time and a signing reason in case any alterations made to the final content. If the certificate is missing or invalid it is recommended to verify the article on the journal website.

## ORIGINAL RESEARCH PAPER

# Chloroplast protease/chaperone AtDeg2 influences cotyledons opening and reproductive development in *Arabidopsis*

Małgorzata Adamiec<sup>1</sup>, Przemysław Jagodzick<sup>1</sup>, Tomasz P. Wyka<sup>2</sup>, Agnieszka Ludwików<sup>3</sup>, Filip Mituła<sup>3</sup>, Lucyna Misztal<sup>1</sup>, Robert Luciński<sup>1</sup>, Grzegorz Jackowski<sup>1\*</sup>

<sup>1</sup> Department of Plant Physiology, Institute of Experimental Biology, Adam Mickiewicz University in Poznań, Umultowska 89, 61-614 Poznań, Poland

<sup>2</sup> Department of General Botany, Institute of Experimental Biology, Adam Mickiewicz University in Poznań, Umultowska 89, 61-614 Poznań, Poland

<sup>3</sup> Department of Biotechnology, Institute of Molecular Biology and Biotechnology, Adam Mickiewicz University in Poznań, Umultowska 89, 61-614 Poznań, Poland

\* Corresponding author. Email: [grzesiek@amu.edu.pl](mailto:grzesiek@amu.edu.pl)

**Abstract**

AtDeg2 is a chloroplast protein with dual protease/chaperone activity. Since data on how the individual activities of AtDeg2 affect growth and development of *Arabidopsis thaliana* plants is missing, two transgenic lines were prepared that express mutated AtDeg2 versions that have either only protease or chaperone activity and a comprehensive ontogenesis stage-based study was performed comprising wild type (WT) plants and insertional mutants that do not express AtDeg2, as well as the two transgenic lines. The repression of both AtDeg2 activities in *deg2-3* mutants altered just a few phenotypic traits including the time when cotyledons were fully opened, the time when 10% flowers were open as well as the number of inflorescence branches and seed length in plants which have completed their generative development. It was demonstrated that complete opening of cotyledons as well as the number of inflorescence branches and seed length in plants which have completed their generative development required involvement of both AtDeg2 activities, whereas the time when 10% of flowers were open was controlled by AtDeg2 protease activity. These results show for the first time that the chaperone activity of AtDeg2 is needed for some elements of generative development of *A. thaliana* plants to proceed normally. So far, the chaperone activity of AtDeg2 was confirmed based on in vitro assays only.

**Keywords**

AtDeg2 chloroplast protein; chaperone; leaf; mutant; ontogenesis; photosynthetic rate; protease; transformant

**Introduction**

Products of five genes identified in the *A. thaliana* nuclear genome encode proteins orthologous to the *E. coli* Deg proteases, namely AtDeg1, 2, 5, 8 and 13, reside exclusively in chloroplasts [1–3]. The AtDeg2 chloroplast protein is a non-ATP hydrolyzing serine endopeptidase peripherally attached to the stromal side of the thylakoid membrane. It belongs to the S1C subfamily of the S1 family (chymotrypsin A, *Bos taurus*) and is classified in the Merops database as “Deg2 chloroplast peptidase (*Arabidopsis thaliana*)”. Recombinant AtDeg2 was shown to catalyze the in vitro hydrolysis of various artificial protein substrates including gelatin [4],  $\beta$ -casein [5,6], and fluorescence-labeled casein [7] indicating that AtDeg2 is a bona fide proteolytic enzyme. The mature AtDeg2 molecule

contains a protease domain with a catalytic H159 D190 S268 triad, as well as PDZ1 and PDZ2 domains that, along with the protease domain, participate in the hexamerization of single AtDeg2 molecules. Furthermore, PDZ domains remodel the proteolytically inactive hexamer into enzymatically competent 12-mers or 24-mers in an allosteric mode after binding of a protein substrate [5]. Besides being a protease, AtDeg2 also has a chaperone activity. Specifically, this protein is able to inhibit the aggregation of denatured lysozyme in vitro [5,6] and can cause in vitro disaggregation of pre-existing aggregates of denatured lysozyme [6]. We have shown that the PDZ2 domain is required both for the chaperone and protease activities of AtDeg2, whereas PDZ1 contributes to the chaperone but not to the protease activity of AtDeg2. The protease domain – but not S268 in its catalytic center – was demonstrated to contribute to AtDeg2 chaperone activity [6]. AtDeg1, another non-ATP hydrolyzing chloroplast protease that belongs to the Deg group, was shown to have a chaperone (refoldase) activity as well, which probably requires protease domain because substitution of the proteolytically active serine residue (S280) by the proteolytically inactive alanine residue (A) considerably reduced the refoldase activity of AtDeg1. It was suggested that AtDeg1 refoldase activity might include assisting in PSII assembly by interacting with the PsbD (D2) protein [8].

There is some information on the physiological functions of AtDeg2 in vivo when plants are grown under nonstress conditions. Notably, in studies carried out using insertional null mutants (*deg2-2* and *deg2-3*), the AtDeg2 protein was found to be required for the morphology of older (juvenile) leaves; the lack of AtDeg2 resulted in juvenile leaf area reduction by half in 3–4-week-old mutant plants, in comparison to WT [9]. Furthermore, AtDeg2 is involved in chloroplast senescence program, since 4-week-old *deg2* mutants did not display senescence-related undulations of chloroplast envelope and thylakoids and had less plastoglobules per chloroplast cross section compared to WT plants [9]. In addition, highly conserved *cis*-regulatory elements specific for transcription factors engaged in leaf senescence and carotenogenesis have been identified in the *AtDEG2* promoter [10]. However, no comprehensive studies of the role of AtDeg2 in *A. thaliana* plant growth and development have been reported and no efforts were undertaken to discriminate between individual roles of protease and chaperone activities of AtDeg2 in controlling chronological progression of stages in plant ontogenesis. To fill this gap in our understanding of the role played by AtDeg2 – a chloroplast protein having dual protease/chaperone activity – the analysis of individual influence of protease and chaperone activities of AtDeg2 on selected phenotypic traits in *Arabidopsis*, including the chronological progression of plant vegetative and generative development, morphology of fully expanded, mature leaves, and of plant organs which have completed their generative development, as well as photosynthetic responses to irradiance and CO<sub>2</sub> concentration, was undertaken. This comprehensive phenotypic screen included WT plants, the insertional mutant *deg2-3* [9], and two transgenic lines that express AtDeg2 variants with either the protease or chaperone activity. The transformants either expressed AtDeg2 without the PDZ1 domain and a C-terminal GFP tag (*35S:AtDEG2<sup>ΔPDZ1</sup>-GFP*) that lacked chaperone activity but was proteolytically active [6], or AtDeg2 with a C-terminal GFP tag that lacked its proteolytic activity but still had its chaperone function (*35S:AtDEG2<sup>S268G</sup>-GFP*) [6]. To make the results plausible, the data concerning phenotypic traits were collected so that the mutants, the transformants, and WT plants represented identical ontogenetic stages, rather than identical age, as had been reported previously [9]. Our results show that both the protease and chaperone activities of AtDeg2 are necessary for cotyledon opening and plant generative development to proceed correctly under nonstress growth conditions.

## Material and methods

### Plant material and growth conditions

Seeds of *A. thaliana* ecotype Columbia plants, *deg2-3* mutants [9], as well as two transgenic lines: *35S:AtDEG<sup>S268G</sup>-GFP* 3.313 and *35S:AtDEG<sup>ΔPDZ1</sup>-GFP* 4.31 were sown on sphagnum peat moss and wood pulp (Agro Wit, Poland) and grown under long-day conditions in an identical manner as described previously [11].

## Plasmid construction

The vector constructs for stable plant transformation (*35S:AtDEG2<sup>S268G</sup>-GFP* and *35S:AtDEG2<sup>ΔPDZ1</sup>-GFP*) were prepared using Gateway technology. The *AtDEG2* coding sequence was amplified by PCR (5'-CACCATGGCCGCCTCCGTAG and 5'-TGCCCA-CACCAGTCCATCAAAGC), while the *DEG2* ΔPDZ1 fragment was chemically synthesized by Thermo Fisher Scientific (USA). Both sequences were subcloned into the pENTR/SD/D-TOPO vector (Invitrogen, USA) and then recombined with the pEarleyGate 103 vector [12] using Gateway LR Clonase II Enzyme Mix (Invitrogen). Site-directed mutagenesis of *AtDEG2* was performed using a QuikChange II XL Site-Directed Mutagenesis Kit (Agilent, USA) according to the manufacturer's protocol, and the following oligonucleotides: 5'-CCAGGGAATGGTGGTGGCCCT and 5'-AGGGC-CACCATTCCCTGG. The *A. thaliana deg2-3* mutant was transformed with the vector constructs by the floral dip method using *Agrobacterium tumefaciens* strain LBA4404 as the host. Transformed seeds were selected on MS media containing the glufosinate ammonium herbicide (10 mg/L).

## Isolation of chloroplast lysates, SDS-PAGE, immunoblotting, quantitation of immunostained bands and antibodies

Chloroplasts were prepared from leaves of WT plants, *deg2-3* mutants, and two transformants at the secondary stage 6.0 of ontogenesis, as described [13]. The chloroplast lysates were prepared by suspending pelleted chloroplasts in a buffer containing 50 mM Hepes-KOH, pH 7.8 and 10 mM MgCl<sub>2</sub>. The equal amounts of protein from the lysates were separated by SDS-PAGE, electrotransferred onto PVDF membranes, and immunostained with primary antibodies raised against the Deg2 apoprotein. The quantification of immunostained bands was performed using the ChemiDoc Imaging System (BioRad, USA) and Gelix One 1d Software ver. 4.1 (Biostep, Germany). The primary antibody against Deg2 (rabbit) was custom-produced (GenScript, USA) using the C-terminal sequence TQALDQGIGDSPVS as the antigen.

## Chronological progression of selected principal and secondary stages of ontogenesis in WT plants, *deg2-3* mutants, and transformants, morphology of plants which have completed a generative development and morphology of fully expanded, mature eighth leaves

Chronological progression of the four principal stages of the plants' ontogenesis was defined in compliance with the BBCH scale aligned for *Arabidopsis* phenotypes [14,15]. These stages are leaf development (Stage 1), inflorescence emergence (Stage 5), flower production (Stage 6), and silique ripening (Stage 8) [11]. The rosette growth (principal Stage 3) was analyzed as described [15].

Chronological progression of leaf development (principal Stage 1) and its secondary stages (1.0 and 1.2–1.9), corresponding to the time of opening of cotyledons and the successive appearance of nine rosette leaves was analyzed by visual inspection of seedlings and plants two times each day.

Chronological progression of principal Stage 3 (rosette growth) and its secondary stages (3.2, 3.5, 3.7, and 3.9, corresponding to the time when the rosette reached 20%, 50%, 70%, and 100% of its final size, respectively) was analyzed by taking digital photographs of the plants two times a day and analyzing the images with ImageJ open source image processing software.

Chronological progression of inflorescence emergence (principal Stage 5) and its only secondary Stage 5.0, which corresponds to the time when the first flower bud appeared, was analyzed by visual inspection of plants two times a day.

Chronological progression of flower production (principal Stage 6) and its secondary Stages 6.0, 6.1, 6.5, and 6.9 which correspond to the time when the first flower as well as 10%, 50%, and 100% of flowers opened, respectively, was analyzed by visual inspection of plants, executed two times a day.

Chronological progression of principal Stage 8 (silique ripening) and its secondary stages (8.0, 8.1, 8.5, and 8.9 corresponding to the time when the first silique as well as 10%, 50%, and 100% of siliques shattered, respectively) was analyzed by visual inspection of plants two times a day.

The height of the shoot, number of inflorescence branches, and number of seeds per plant were determined by visual inspection of plants that had reached secondary Stage 8.9 of ontogenesis (100% siliques shattered).

Whole, mature, eighth leaves were studied at the moment when they had reached their final size (i.e., close to the time when plant ontogenesis reached the 6.1 secondary stage). The leaves were digitally scanned using an Epson Perfection V700 Photo scanner (Epson, Indonesia) and the images were analyzed with WinFolia Software ver. 2012a (Regent Instruments Inc., Canada). The leaf length, width and area were automatically determined by the software. The leaf shape coefficient was calculated as described by Kincaid et al [16].

### Microscopy

Seeds were collected at the moment when plants had reached secondary Stage 8.9 of ontogenesis (100% siliques shattered). Scanning electron microscopy of the seeds (EVO 40; Carl Zeiss Microscopy GMBH, Germany) was performed following Western et al. [17]. The negative scanning and digital image analysis was performed as previously described [9].

### Gas exchange analysis

Gas exchange measurements were conducted using the Li-6400XT photosynthesis system equipped with the standard 6-cm<sup>2</sup> chamber and a red-and-blue light source (Li-Cor Inc., USA). Individual leaf (eighth leaf of the plant, at the time of reaching full size) was enclosed in the chamber and tape was used to improve seal. Leaf temperature was maintained at 22°C within the chamber. After acclimation in the chamber, leaf responses to irradiance were determined by varying photosynthetic photon flux density in 1,200, 1,000, 800, 600, 500, 400, 300, 250, 200, 150, 100, 75, 50, 25, 0  $\mu\text{mol m}^{-2} \text{s}^{-1}$  steps while maintaining the concentration of CO<sub>2</sub> at 400  $\mu\text{mol mol}^{-1}$ . Next, irradiance was restored to 1,200  $\mu\text{mol m}^{-2} \text{s}^{-1}$  and, when photosynthetic rate (A) returned to the initial level, an A/C<sub>i</sub> response curve was generated by taking measurements under the ambient CO<sub>2</sub> levels of: 400, 300, 200, 150, 100, 75, 50  $\mu\text{mol mol}^{-1}$ , followed by 400, 500, 600, 750, 1,000, 1,400, and 1,800  $\mu\text{mol mol}^{-1}$  CO<sub>2</sub>. Leaf area was determined using a flatbed Epson Perfection V700 Photo scanner and WinFolia Software. Photosynthetic rates and internal leaf concentrations of CO<sub>2</sub> (C<sub>i</sub>) were calculated with the inbuilt Li-6400XT software. Sigma Plot 11 (Systat Software, USA) was used to fit photosynthetic model equations to empirical data. A nonrectangular hyperbola model of photosynthesis [18] was fitted to light response data and maximal light saturated photosynthesis (A<sub>max</sub>), dark respiration (R<sub>d</sub>), curvature factor (Θ), and quantum yield of photosynthetic CO<sub>2</sub> assimilation (Φ) were estimated. Two phase model of photosynthesis [19] was fitted to the A/C<sub>i</sub> measurements assuming that data points with C<sub>i</sub> < 400  $\mu\text{mol mol}^{-1}$  represented photosynthesis that was limited by amount, activity or kinetics of Rubisco, whereas those with C<sub>i</sub> > 400  $\mu\text{mol mol}^{-1}$  represented photosynthesis limited by the rate of electron transport required for the regeneration of ribulose 1,5-biphosphate (RuBP) [20]. Kinetic parameters of Rubisco were taken from Long and Bernacchi [21], and the maximal carboxylation rate of Rubisco (V<sub>c,max</sub>) and maximal electron transport rate (J<sub>max</sub>) were estimated as model parameters. Both parameters were normalized to 25°C using the Sharkey spreadsheet [22].

### Statistical analysis

Statistical significance of the differences in phenotypic parameters was analyzed with the Student's *t* test at *p* < 0.05. Prior to the Student's *t* test analysis, the data were tested

for distribution normality with the Shapiro–Wilk test and the equality of variances was established with the *F* test.

Parameters produced by analysis of *A*/PPFD (photosynthetic photon flux density) and *A*/*C*<sub>i</sub> response curves were compared between the genotypes with an unequal-variance Student's *t* tests using the JMP 8.0.2 statistical package (SAS Institute, USA).

## Results

### Stable transformants

To dissect the roles of AtDeg2 chaperone and protease activities in the establishment of selected phenotypic traits, we prepared *Arabidopsis* transgenic lines in the *deg2-3* [9] background that express mutant alleles of AtDeg2 under the control of the 35S cauliflower mosaic virus promoter. Two types of transgenic plants were generated: (*i*) Deg2<sup>S268G</sup> transgenic plants expressing the mutant protein-GFP fusion that is active as a chaperone but devoid of its protease activity, and (*ii*) Deg2<sup>ΔPDZ1</sup> transgenic plants expressing mutant protein-GFP fusion that is proteolytically active but devoid of chaperone activity. Eight lines for each of the two types of transgenic plants were selected and all sixteen lines were screened for the presence of the transgene by genomic PCR (data not shown). For further experiments, two lines were selected (*35S:AtDEG2<sup>S268G</sup>-GFP 3.313* and *35S:AtDEG2<sup>ΔPDZ1</sup>-GFP 4.31*) for which the abundance of AtDeg2-GFP fusion proteins was demonstrated to be the most similar to the abundance of native AtDeg2 in WT plants (Fig. 1).

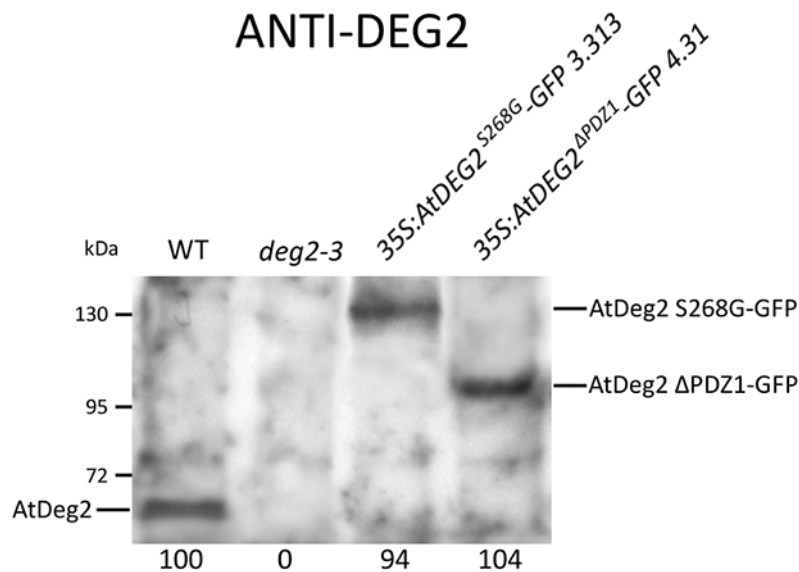


**Fig. 1** Immunoblot analysis of the protein levels of AtDeg2 and AtDeg2-GFP fusions in WT plants, *deg2-3* mutants, *35S:AtDEG2<sup>S268G</sup>-GFP 3.313* and *35S:AtDEG2<sup>ΔPDZ1</sup>-GFP 4.31* transgenic lines stably expressing mutated versions of AtDeg2. Protein samples of chloroplast lysates from leaves of plants at the secondary Stage 6.0 of ontogenesis [14] were resolved by SDS-PAGE, electrotransferred onto PVDF membranes, and immunolabeled with Anti-Deg2 antibodies. The levels of AtDeg2 or AtDeg2-GFP fusions, quantified relative to the values of AtDeg2 in WT plants (100%), are indicated under the corresponding lanes.

### Chronological progression of ontogenetic stages in WT plants, *deg2-3* mutants, and transgenic lines

To investigate the role of AtDeg2 in the chronological progression of plant vegetative and generative development, selected principal and secondary stages in plant ontogenesis from the opening of cotyledons to fruit ripening were studied for WT plants, *deg2-3*

mutants that did not exhibit protease nor chaperone activity, and the two transgenic lines expressing the protein fusions. The time (in days) required for individual secondary stages to be completed in WT plants and *deg2-3* mutants are displayed in Tab. 1. In the vast majority of cases there were no alterations in chronological progression of the secondary ontogenesis stages as far as WT/*deg2-3* comparison is concerned, however, the time needed for secondary Stages 1.0 and 6.1 (cotyledons fully opened and 10% of flowers opened, respectively) to complete was different between the WT and *deg2-3* null mutant plants. To distinguish between the AtDeg2 protease and chaperone activities during the chronological progression of 1.0 and 6.1 secondary stages of ontogenesis, the transformants were introduced into this part of the study and the results are shown in Tab. 2. The cotyledons became fully opened about half a day later in *deg2-3* mutants than in WT plants and a similar, significant delay was observed in the both transgenic lines as well. Since there were no significant differences in this respect between *deg2-3* mutants and transgenic lines, both the protease and chaperone activities of AtDeg2 are necessary for cotyledon opening to proceed at an appropriate rate. The 6.1 secondary stage occurred significantly earlier in *deg2-3* mutants (in 26th day) than in WT plants (30th day). Plants representing 35S:*AtDEG2*<sup>S268G</sup>-*GFP* 3.313 line behaved similarly to the *deg2-3* mutants, while 35S:*AtDEG2*<sup>APDZ1</sup>-*GFP* 4.31 ones did not differ from WT plants and this indicates that the protease activity of AtDeg2 is needed to reach the secondary Stage 6.1 of ontogenesis at the right time.

**Tab. 1** Analysis of chronological progression of principal ontogenetic Stages 1, 3, 5, 6, and 8 in WT plants and *deg2-3* mutants.

Principal stage	Secondary stage	Time required to accomplish the secondary stage (days ±SD)	
		WT	<i>deg2-3</i>
1 (leaf development)	1.0 – cotyledons fully opened	2.52 ±0.22	2.95 ±0.19*
	1.2 – 2 rosette leaves > 1 mm	7.00 ±0.64	7.00 ±0.68
	1.3 – 3 rosette leaves > 1 mm	9.70 ±1.01	9.75 ±0.93
	1.4 – 4 rosette leaves > 1 mm	10.10 ±1.04	10.25 ±0.93
	1.5 – 5 rosette leaves > 1 mm	11.20 ±1.17	11.15 ±1.27
	1.6 – 6 rosette leaves > 1 mm	12.05 ±1.09	11.95 ±1.41
	1.7 – 7 rosette leaves > 1 mm	14.45 ±1.20	14.75 ±1.53
	1.8 – 8 rosette leaves > 1 mm	15.58 ±1.51	15.79 ±1.29
	1.9 – 9 rosette leaves > 1 mm	16.63 ±1.23	16.83 ±1.40
3 (rosette growth)	3.2 – rosette reaches 20% of its final size	17.41 ±1.46	16.88 ±1.72
	3.5 – rosette reaches 50% of its final size	20.74 ±1.82	20.68 ±1.94
	3.7 – rosette reaches 70% of its final size	22.02 ±1.78	22.01 ±2.12
	3.9 – rosette reaches 100% of its final size	24.22 ±1.92	25.13 ±2.28
5 (inflorescence emergence)	5.1 – first flower bud visible	23.76 ±1.94	23.76 ±1.51
6 (flower production)	6.0 – first flower opened	24.00 ±1.10	23.90 ±1.29
	6.1 – 10% flowers to be produced have opened	30.00 ±2.26	26.00 ±2.47*
	6.5 – 50% flowers to be produced are opened	39.00 ±1.98	37.00 ±2.12
	6.9 – flowering complete	72.00 ±2.12	74.00 ±2.47
8 (silique ripening)	8.0 – first silique shattered	41.70 ±1.87	42.20 ±2.28
	8.1 – 10% siliques to be produced have shattered	46.50 ±2.34	46.50 ±2.77
	8.5 – 50% siliques to be produced have shattered	59.00 ±2.56	57.50 ±2.83
	8.9 – 100% siliques have shattered	86.50 ±2.86	87.50 ±3.22

The asterisks indicate the data for which the differences between WT plants and *deg2-3* mutants were significant at  $p < 0.05$  ( $N = 40$ ).

**Tab. 2** Analysis of chronological progression of secondary ontogenetic Stages 1.0 and 6.1 in WT plants, *deg2-3* mutants, as well as plants representing *35S:AtDEG2<sup>S268G</sup>-GFP 3.313* and *35S:AtDEG2<sup>APDZ1</sup>-GFP 4.31* transgenic lines.

Secondary stage	Time required to accomplish the secondary stage (days $\pm$ SD)			
	WT	<i>deg2-3</i>	<i>35S:AtDEG2<sup>S268G</sup>-GFP 3.313</i>	<i>35S:AtDEG2<sup>APDZ1</sup>-GFP 4.31</i>
1.0	2.52 $\pm$ 0.22 <sup>b,c,d</sup>	2.95 $\pm$ 0.19 <sup>a</sup>	3.10 $\pm$ 0.28 <sup>a</sup>	3.20 $\pm$ 0.31 <sup>a</sup>
6.1	30.00 $\pm$ 2.26 <sup>b,c</sup>	26.00 $\pm$ 2.47 <sup>a,d</sup>	26.00 $\pm$ 2.86 <sup>a,d</sup>	32.00 $\pm$ 3.21 <sup>b,c</sup>

The letters a, b, c, and d indicate the data for which any genotype/WT plants, any genotype/*deg2-3* mutants, any genotype/*35S:AtDEG2<sup>S268G</sup>-GFP 3.313* transformants, and any genotype/*35S:AtDEG2<sup>APDZ1</sup>-GFP 4.31* transformants differences, respectively, were significant ( $p < 0.05$ ,  $N = 40$ ).

### Morphology of plants that have completed their generative development

As AtDeg2 was demonstrated to regulate, at least transiently, the generative development of plant, namely secondary Stage 6.1 (Tab. 1), a few selected features of plants that have completed their generative development (secondary Stage 8.9) were studied. These features included the height of the shoot, number of inflorescence branches, number of seeds per plant, and length of the seed (it was checked that time the transformants needed to complete 8.9 secondary stage was 85 and 86 days, for *35S:AtDEG2<sup>S268G</sup>-GFP 3.313* and *35S:AtDEG2<sup>APDZ1</sup>-GFP 4.31* lines, respectively, and did not differ from those indicated for WT plants and *deg2-3* mutants in Tab. 1). Whenever the differences between WT and *deg2-3* were significant, the data for the transgenic plants are shown as well, while in remaining cases only WT and *deg2-3* data are displayed (Fig. 2).

Two significant WT/*deg2-3* alterations were recorded, involving the number of inflorescence branches and length of the seed. Namely, the number of inflorescence branches was lower in *deg2-3* in comparison to WT plants giving the mutants less bushy appearance. There were no significant differences in this respect among *deg2-3* mutants and the transformants indicating the necessity of both AtDeg2 protein activities for plants to produce normal inflorescence branching. Seeds from *deg2-3* plants were significantly longer than those from WT plants but no differences were observed between the *deg2-3* mutants and the transformants. Thus these results suggest that both AtDeg2 activities are necessary for seeds to reach correct length.

### Morphology of fully expanded mature leaves

We previously reported that AtDeg2 controls the area of juvenile leaves but does not impact the area of mature rosette leaves of 4-week-old plants [9], i.e., when mature leaves were still growing but juvenile leaves have finished their expansion [11]. We now wanted to know whether the fully expanded mature leaves follow the same trend. In preliminary experiments, it was found that the eighth (mature) leaves of WT plants, the mutants, the transformant lines *35S:AtDEG2<sup>S268G</sup>-GFP 3.313* and *35S:AtDEG2<sup>APDZ1</sup>-GFP 4.31* reached their final size at the day 30th, 29th, 29th, and 31st, respectively (data not shown), i.e., very close to the 6.1 secondary stage of ontogenesis (10% flowers opened). The morphological properties of fully expanded eighth leaves of WT plants and *deg2-3* mutants are shown in Fig. 3.

No significant differences were observed between WT and *deg2-3* plants, thus AtDeg2 does not seem to be linked to the morphology of fully expanded mature leaves.

### A/C<sub>i</sub> and light response curves of fully expanded mature leaves

Since it was reported that various chloroplast proteases, including those belonging to the Deg group, had significantly contributed to photosynthetic efficiency and capacity in leaves [23–25], A/C<sub>i</sub> and light response curves for mature (eighth) leaves were studied at the moment when the leaves reached their final size. Results of the A/C<sub>i</sub> response analysis showed that *deg2-3* mutants did not differ significantly from WT  $V_{c,max}$  or  $J_{max}$

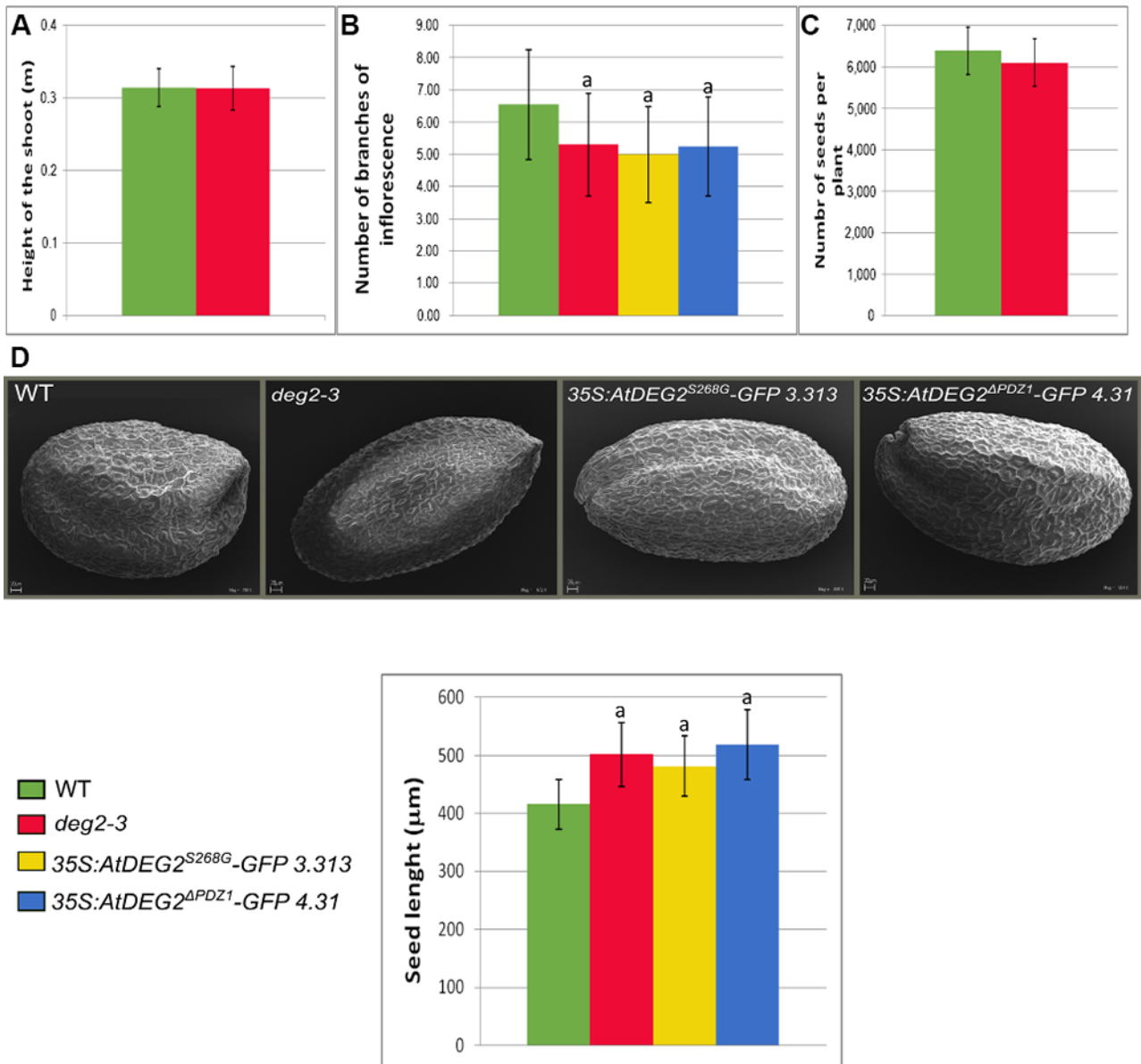


**Fig. 2** Analysis of morphological traits of plants that completed their generative development. Height of the shoot (A), number of inflorescence branches (B), and number of seeds per plant (C) were measured for WT plants, *deg2-3* mutants, as well as plants of *35S:AtDEG2<sup>S268G</sup>-GFP 3.313* and *35S:AtDEG2<sup>ΔPDZ1</sup>-GFP 4.31* transgenic lines at the 8.9 secondary stage of ontogenesis (100% siliques shattered). Seeds from WT plants, *deg2-3* mutants, *35S:AtDEG2<sup>S268G</sup>-GFP 3.313* and *35S:AtDEG2<sup>ΔPDZ1</sup>-GFP 4.31* transgenic lines were collected from plants that had reached the secondary Stage 8.9, were imaged by scanning electron microscopy and measured (D). Values are represented as the mean  $\pm$ SD ( $N = 40$ ). The letters *a* indicate the data for which any genotype/WT plants differences were significant ( $p < 0.05$ ).

values (Fig. 4). Furthermore, leaves from WT plants and *deg2-3* mutants exhibited very similar light response curves with no statistically significant differences in maximal photosynthetic rate  $A_{max}$ , dark respiration  $R_d$ , quantum yield of photosynthetic  $CO_2$  assimilation  $\Phi$ , or curvature factor  $\Theta$  (Fig. 5).

## Discussion

To gain an insight into the significance of AtDeg2 protease and chaperone activities for the growth and development of *A. thaliana* plants under nonstress growth conditions, two transformant lines were obtained which express mutated AtDeg2-GFP fusion proteins that have either only chaperone (*35S:AtDEG2<sup>S268G</sup>-GFP 3.313*) or only protease (*35S:AtDEG2<sup>ΔPDZ1</sup>-GFP 4.31*) activity (Fig. 1). These lines were examined in parallel with



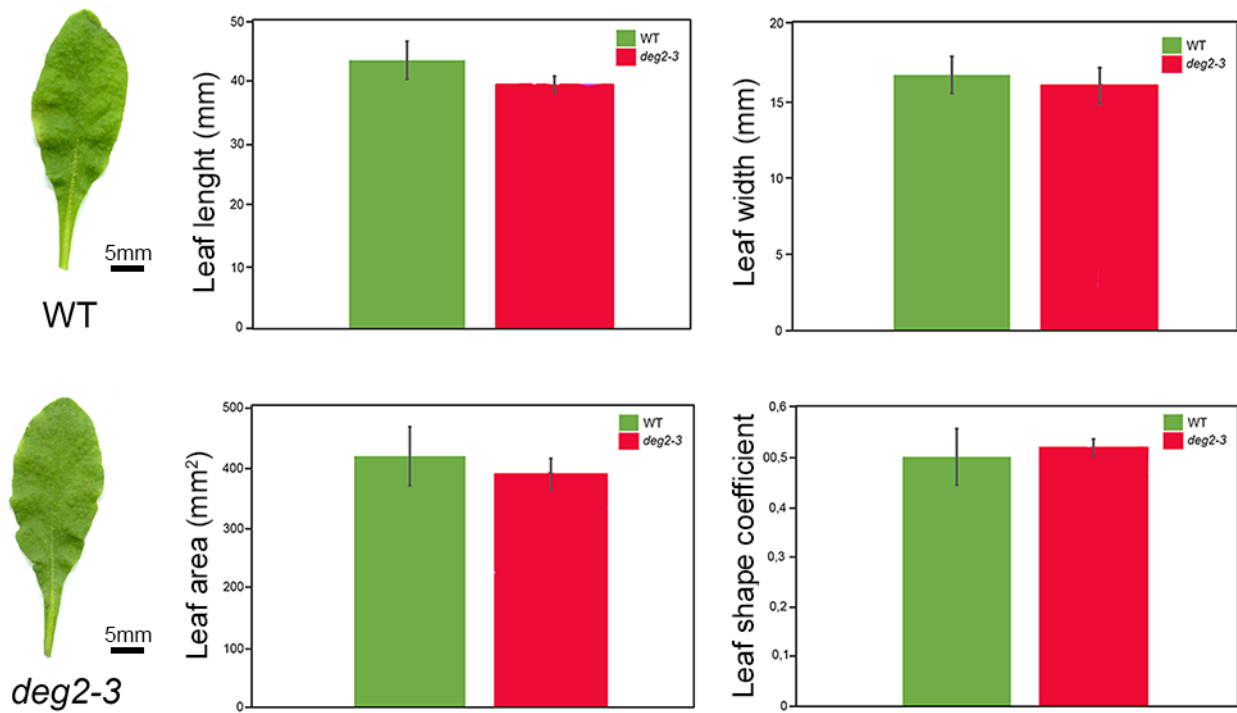


**Fig. 3** Morphological analysis of fully expanded, mature (eighth) leaves from WT plants and *deg2-3* mutants. The leaves were digitally scanned and leaf length, width, area, and shape coefficient were determined by image analysis. Values are mean  $\pm$ SD ( $p < 0.05$ ,  $N = 40$ ).

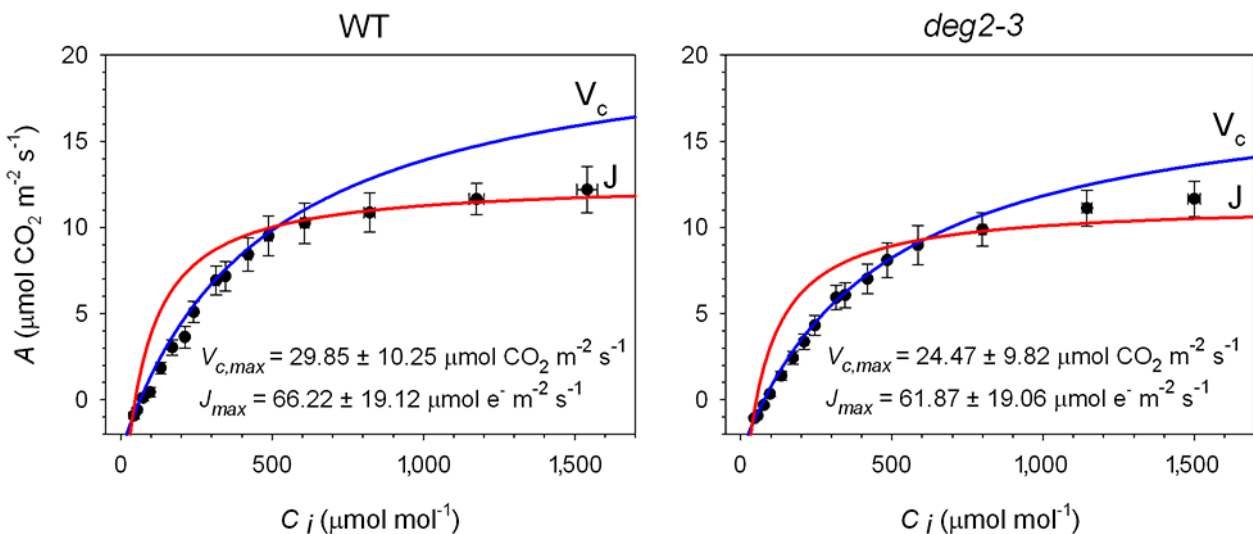


**Fig. 4** Responses of photosynthetic rate ( $A$ ) to internal concentration of  $\text{CO}_2$  ( $C_i$ ) in fully expanded, mature (eighth) leaves of WT plants ( $N = 6$ ) and *deg2-3* mutants ( $N = 12$ ). Points represent mean values ( $\pm$ SE) and curves are plots of the photosynthesis model equations [19] using average parameters obtained by fitting the model to individual plant data. Data points where  $C_i < 400 \mu\text{mol mol}^{-1}$  represent Rubisco limited photosynthesis (blue line; marked “Vc”) and points where  $C_i > 400 \mu\text{mol mol}^{-1}$  represent photosynthesis limited by the rate of RuBP regeneration (red line; marked “J”). Estimated means ( $\pm$ SD) indicate the maximal Rubisco carboxylation rate ( $V_{c,max}$ ) and maximal rate of photosynthetic electron transport ( $J_{max}$ ) standardized to 25°C are shown in respective panels.

WT plants and *deg2-3* null mutants [9]. Our results indicate that AtDeg2 is involved in regulating the time it takes for cotyledons to fully open (both activities engaged; Tab. 1 and Tab. 2), the time when 10% of the flowers became open (protease activity engaged only; Tab. 1, Tab. 2), as well as the accomplishment of normal inflorescence branching and normal seed length in plants which have completed their generative development (both activities engaged; Fig. 2). Red light-controlled opening of cotyledons was shown to involve an unidentified MKKK(s)–MKK10–MPK6 cascade. Active MPK6 is thought

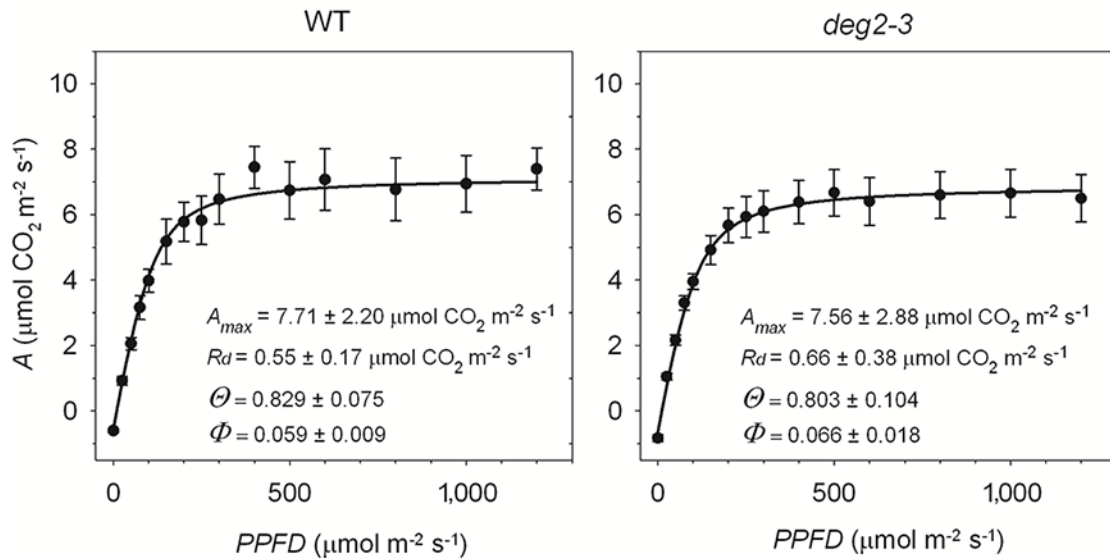


**Fig. 5** Responses of photosynthetic rate ( $A$ ) to photosynthetic photon flux density (PPFD) in fully expanded, mature (eighth) leaves of WT ( $N = 7$ ) and *deg2-3* mutant plants ( $N = 11$ ). Points are mean values ( $\pm SE$ ) and curves are plots of the nonrectangular hyperbola equation [18] using average parameters obtained by fitting the equation to individual plant data. Estimated means ( $\pm SD$ ) model the parameters: maximal light saturated photosynthetic rate ( $A_{max}$ ), respiration rate in the dark ( $R_d$ ), curvature factor ( $\Theta$ ), and quantum yield of photosynthetic  $CO_2$  assimilation ( $\Phi$ ), which are shown in respective panels.

to phosphorylate the PIF3 transcription factor, accelerate its degradation, and regulate expression of PIF3-responsive genes in this way – to promote cotyledon opening [26]. *AtDEG2* is extensively expressed in fully opened cotyledons as judged by the results of the application of the eFP browser tool [27]. It seems that a crosstalk may exist between the signaling pathways involved in the opening of cotyledons and AtDeg2-regulated pathways. It is regarded that the key factors controlling the vegetative to reproductive growth change in *A. thaliana* are *miR156* and *miR172* [28]; *miR156* delays the induction of generative development by limiting the accumulation of *SPL* transcription factors that act as flowering promoters [29], while *miR172* accelerates flowering time, inter alia, by downregulating the abundance of mRNA encoding flowering repressors, such as the *AP2* group of transcription factors [30]. Since it was demonstrated by us in this work that AtDeg2 – acting as a protease – regulated the time necessary for 10% of flowers to become fully open (Tab. 1, Tab. 2), we suggest that AtDeg2 regulates the turnover of a chloroplast protein that has a functional link with flowering repressors and/or promoters turnover. Other AtDeg proteases may have similar function as suggested by the ability of AtDeg5 to regulate flower production (secondary Stage 6.5 of ontogenesis) [11].

AtDeg2 was hereby shown to regulate the development of normal inflorescence branching and normal seed length in plants that have completed their generative development through both its protease and chaperone activity. Therefore, it may be proposed that a crosstalk exists between the signaling pathways for the establishment of inflorescence branching and seed dimensions, and the turnover of AtDeg2-regulated chloroplast proteins and pathways encompassing AtDeg2 chaperone potency (control of chloroplast proteins biogenesis?). In *A. thaliana*, lateral inflorescence branching was shown to be controlled by genes encoding *API*, *LFY*, and MADS-box transcription factors, with a key role of cytokinins [31,32]. In turn, seed size is coordinately controlled by signaling pathways involving *IKU1*, *IKU2*, *SHB1*, and *MINI3* genes as well as the ubiquitin–proteasome 26S pathway, G-protein signaling, and the mitogen-activated protein kinase signaling pathway (for a review see [33]).

We demonstrate herein that WT plants and *deg2-3* mutants do not have significant differences in the morphological properties of fully expanded mature (eighth) rosette leaves (Fig. 3). This finding, coupled with the determination that AtDeg2 did not affect morphological traits in expanding mature rosette leaves [9], indicates that neither of the

two AtDeg2's activities influences mature leaf growth throughout the life-span of the plant. Since there were no changes in leaf development (i.e., progression of the appearance of subsequent leaves) found between WT plants and *deg2-3* mutants (Tab. 1), the reduction of area of fully expanded third and fourth juvenile leaves in *deg2-3* mutants compared to WT plants [9] was not due to the delay in their appearance.

The photosynthetic parameters of fully expanded mature (eighth) rosette leaves – estimated based on A/C<sub>i</sub> and light response curves – remained unaffected by loss of both AtDeg2 activities (Fig. 4 and Fig. 5).

AtDeg1 is the only other protease that belongs to the Deg group that also has demonstrated chaperone (refoldase) activity in vitro [8]; however, it was not analyzed in terms of significance of its chaperone (or protease) activity for plant growth and development. Our results show for the first time that under nonstress growth conditions, AtDeg2, another chloroplast-targeted protease belonging to Deg group, influences some phenotypic features of *A. thaliana* plants through its chaperone activity, in conjunction with its protease activity. However, the number of phenotypic features in *A. thaliana* plants that are influenced by the protease or dual protease/chaperone activities of AtDeg2 is low and entirely consistent with the observation that AtDeg2 loss does not have an impact on the reproductive fitness of individual plants (Fig. 2). Thus, we suggest that the principal function of AtDeg2 may be most important in stress conditions, as exemplified by its involvement in stress-related degradation of damaged Lhcb6 apoprotein [9].

## References

1. Lipińska B, Sharma S, Georgopoulos C. Sequence analysis and regulation of the *htrA* gene of *Escherichia coli*: a sigma 32-independent mechanism of heat-inducible transcription. *Nucleic Acids Res.* 1988;16(21):10053–10067. <https://doi.org/10.1093/nar/16.21.10053>
2. Strauch KL, Beckwith J. An *Escherichia coli* mutation preventing degradation of abnormal periplasmic proteins. *Proc Natl Acad Sci USA.* 1988;85(5):1576–1580. <https://doi.org/10.1073/pnas.85.5.1576>
3. Tanz SK, Castleden I, Hooper CM, Small I, Millar AH. Using the SUBcellular database for *Arabidopsis* proteins to localize the Deg protease family. *Front Plant Sci.* 2014;5:396. <https://doi.org/10.1074/jbc.M108575200>
4. Haussühl K, Andersson B, Adamska I. A chloroplast DegP2 protease performs the primary cleavage of the photodamaged D1 protein in plant photosystem II. *EMBO J.* 2001;20(4):713–722. <https://doi.org/10.1093/emboj/20.4.713>
5. Sun R, Fan H, Gao F, Lin Y, Zhang L, Gong W, et al. Crystal structure of *Arabidopsis* Deg2 protein reveals an internal PDZ ligand locking the hexameric resting state. *J Biol Chem.* 2012;287(44):37564–37569. <https://doi.org/10.1074/jbc.M112.394585>
6. Jagodzik P, Luciński R, Misztal L, Jackowski G. The contribution of individual domains of chloroplast protein AtDeg2 to its chaperone and proteolytic activities. *Acta Soc Bot Pol.* 2018;87(1):3570. <https://doi.org/10.5586/asbp.3570>
7. Stroher E, Dietz KJ. The dynamic thiol-disulphide redox proteome of the *Arabidopsis thaliana* chloroplast as revealed by differential electrophoretic mobility. *Physiol Plant.* 2008;133(3):566–583 <https://doi.org/10.1111/j.1399-3054.2008.01103.x>
8. Sun XW, Ouyang J, Guo J, Ma J, Lu C, Adam Z, et al. The thylakoid protease Deg1 is involved in photosystem-II assembly in *Arabidopsis thaliana*. *Plant J.* 2010;62(2):240–249. <https://doi.org/10.1111/j.1365-1313X.2010.04140.x>
9. Luciński R, Misztal L, Samardakiewicz S, Jackowski G. The thylakoid protease Deg2 is involved in stress-related degradation of the photosystem II light-harvesting protein Lhcb6 in *Arabidopsis thaliana*. *New Phytol.* 2011;192(1):74–86. <https://doi.org/10.1111/j.1469-8137.2011.03782.x>
10. Jagodzik P, Adamiec M, Jackowski G. AtDeg2 – a chloroplast protein with dual protease/chaperone activity. *Acta Soc Bot Pol.* 2014;83(3):169–174. <https://doi.org/10.5586/asbp.2014.018>

11. Baranek M, Wyka T, Jackowski G. Downregulation of chloroplast protease AtDeg5 leads to changes in chronological progression of ontogenetic stages, leaf morphology and chloroplast ultrastructure in *Arabidopsis*. *Acta Soc Bot Pol*. 2015;84(1):59–70. <https://doi.org/10.5586/asbp.2015.001>
12. Earley KW, Haag JR, Pontes O, Opper K, Juehne T, Song K, et al. Gateway-compatible vectors for plant functional genomics and proteomics. *Plant J*. 2006;45(4):616–629. <https://doi.org/10.1111/j.1365-313X.2005.02617.x>
13. Grabsztunowicz M, Jackowski G. Isolation of intact and pure chloroplasts from leaves of *Arabidopsis thaliana* plants acclimated to low irradiance for studies on Rubisco regulation. *Acta Soc Bot Pol*. 2013;82(1):91–95. <https://doi.org/10.5586/asbp.2012.043>
14. Lancashire PD, Bleiholder H, van den Boom T, Langelüddeke P, Stauss R, Weber E, et al. A uniform decimal code for growth stages of crops and weeds. *Ann Appl Biol*. 1991;119:561–560. <https://doi.org/10.1111/j.1744-7348.1991.tb04895.x>
15. Boyes DC, Zayed AM, Ascenzi R, McCaskill AJ, Hoffman NE, Davis KR, et al. Growth stage-based phenotypic analysis of *Arabidopsis*: a model for high throughput functional genomics in plants. *Plant Cell*. 2001;13(7):1499–1510. <https://doi.org/10.2307/3871382>
16. Kincaid DT, Schneider RB. Quantification of leaf shape with a microcomputer and Fourier transform. *Can J Bot*. 1983;61:2333–2342. <https://doi.org/10.1139/b83-256>
17. Western TL, Skinner DJ, Haughn GW. Differentiation of mucilage secretory cells of the *Arabidopsis* seed coat. *Plant Physiol*. 2000;122(2):345–356. <https://doi.org/10.1104/pp.122.2.345>
18. Lobo F, de Barros MP, Dalmagro HJ, Dalmolin ÂC, Pereira WE, de Souza ÉC, et al. Fitting net photosynthetic light-response curves with Microsoft Excel – a critical look at the models. *Photosynthetica*. 2013;51(3):445–456. <https://doi.org/10.1007/s11099-013-0045-y>
19. Farquhar GD, von Caemmerer S, Berry JA. A biochemical model of photosynthetic CO<sub>2</sub> assimilation in leaves of C<sub>3</sub> species. *Planta*. 1980;149(1):78–90. <https://doi.org/10.1007/BF00386231>
20. Tanaka Y, Sugano SS, Shimada T, Nishimura I. Enhancement of leaf photosynthetic capacity through increased stomatal density in *Arabidopsis*. *New Phytol*. 2013;198(3):757–764. <https://doi.org/10.1111/nph.12186>
21. Long SP, Bernacchi CJ. Gas exchange measurements, what can they tell us about the underlying limitations to photosynthesis? Procedures and sources of error. *J Exp Bot*. 2003;54(392):2393–2401. <https://doi.org/10.1093/jxb/erg262>
22. Sharkey TD. What gas exchange data can tell us about photosynthesis. *Plant Cell Environ*. 2016;39:1161–1163. <https://doi.org/10.1111/pce.12641>
23. Sjögren LL, Stanne TM, Zheng B, Sutinen S, Clarke AK. Structural and functional insights into the chloroplast ATP-dependent Clp protease in *Arabidopsis*. *Plant Cell*. 2006;18(10):2635–2649. <https://doi.org/10.1105/tpc.106.044594>
24. Luciński R, Misztal L, Samardakiewicz S, Jackowski G. Involvement of Deg5 protease in wounding-related disposal of PsbF apoprotein. *Plant Physiol Biochem*. 2011;4(3):311–320. <https://doi.org/10.1016/j.plaphy.2011.01.001>
25. Kim J, Olinares PD, Oh SH, Ghiasaura S, Poliakov A, Ponnala L, et al. Modified Clp protease complex in ClpP3 null mutant and consequences for chloroplast development and function in *Arabidopsis*. *Plant Physiol*. 2013;162(1):157–179. <https://doi.org/10.1104/pp.113.215699>
26. Xin X, Chen W, Wang B, Zhu F, Li Y, Yang H, et al. *Arabidopsis* MKK10–MPK6 mediates red-light-regulated opening of seedling cotyledons through phosphorylation of PIF3. *J Exp Bot*. 2018;69(3):423–439. <https://doi.org/10.1093/jxb/erx418>
27. Winter D, Vinegar B, Nahal H, Ammar R, Wilson GV, Provart NJ. An “electronic fluorescent pictograph” browser for exploring and analyzing large-scale biological data sets. *PLoS One*. 2007;2(8):e718. <https://doi.org/10.1371/journal.pone.0000718>
28. Shrestha R, Gómez-Ariza J, Brambilla V, Fornara F. Molecular control of seasonal flowering in rice, *Arabidopsis* and temperate cereals. *Ann Bot*. 2014;114(7):1445–1458. <https://doi.org/10.1093/aob/mcu032>
29. Wu G, Poethig RS. Temporal regulation of shoot development in *Arabidopsis thaliana* by *miR156* and its target *SPL3*. *Development*. 2006;133(18):3539–3547. <https://doi.org/10.1242/dev.02521>
30. Aukerman MJ, Sakai H. Regulation of flowering time and floral organ identity by

- a microRNA and its *APETALA2*-like target genes. *Plant Cell*. 2003;15(11):2730–2741. <https://doi.org/10.1105/tpc.016238>
31. Liu C, Teo ZW, Bi Y, Song S, Xi W, Yang X, et al. A conserved genetic pathway determines inflorescence architecture in *Arabidopsis* and rice. *Dev Cell*. 2013;24(6):612–622. <https://doi.org/10.1016/j.devcel.2013.02.013>
  32. Han Y, Yiang H, Jiao Y. Regulation of inflorescence architecture by cytokinins. *Front Plant Sci*. 2014;5:669. <https://doi.org/10.3389/fpls.2014.00669>
  33. Li N, Li Y. Signaling pathways of seed size control in plants. *Curr Opin Plant Biol*. 2016;33:23–32. <https://doi.org/10.1016/j.pbi.2016.05.008>